Hydrolysis of Bis((trimethylsilyl)methyl)tin Dihalides. Crystallographic and Spectroscopic Study of the Hydrolysis Pathway†

Jens Beckmann, Markus Henn, Klaus Jurkschat,* and Markus Schürmann

Lehrstuhl für Anorganische Chemie II der Universität Dortmund, 44221 Dortmund, Germany

Dainis Dakternieks and Andrew Duthie

Centre for Chiral and Molecular Technologies, Deakin University, Geelong 3217, Australia

Received August 6, 2001

The synthesis and characterization by multinuclear NMR spectroscopy of the diorganotin dihalides $(Me_3SiCH_2)_2SnX_2$ (**1**, X = Cl; **2**, X = Br), the diorganotin dichloride water adduct $(Me_3SiCH_2)_2SnCl_2{\cdot}H_2O$ (**1a**), the dimeric tetraorganodistannoxanes $[(Me_3SiCH_2)_2(X)SnOSn(Y)(CH_2SiMe_3)_2]_2$ (**3**, X = Y = Cl; **4**, X = Br, Y = OH; **5**, X = Br, Y = F; **6**, X = Y = OH; **8**, X = Cl, Y = OH), and the molecular diorganotin oxide *cyclo*-$[(Me_3SiCH_2)_2SnO]_3$ (**7**) are reported. The structures in the solid state of compounds **1a**, **3**, **6**, and **7** were determined by single-crystal X-ray analysis. In toluene solution, the hydroxy-substituted tetraorganodistannoxane **6** is in equilibrium with the diorganotin oxide **7** and water. The eight-membered diorganotin oxide *cyclo*-$[(Me_3SiCH_2)_2SnO]_4$ (**7a**) is proposed to be involved in this equilibrium. On the basis of the results of this and previous works, a general hydrolysis pathway is developed for diorganotin dichlorides containing reasonably bulky substituents.

Introduction

The hydrolysis of diorganotin dihalides R_2SnX_2 (R = alkyl, aryl; X = Cl, Br) has been the subject of several works in the past. In pioneering work, Rochow and Seyferth[1] and later Tobias and co-workers[2−7] have studied the hydrolysis of diorganotin dichlorides containing small organic substituents in aqueous medium. These studies revealed a number of cationic, neutral, and anionic diorganotin species in aqueous solution, such as $[R_2Sn]^{2+}$, $[R_2SnOH]^+$, $[(R_2Sn)_2(OH)_2]^{2+}$, $[(R_2Sn)_2(OH)_3]^+$, $R_2Sn(OH)_2$, and $[R_2Sn(OH)_3]^-$ (R = Me, Et). More recently, Rizzarelli and co-workers revisited the specification of these species and systematically determined their stability constants and their distribution in solution depending on the pH value.[8]

Furthermore, the preparative hydrolysis of diorganotin dihalides in organic solvents with aqueous base (two-layer reaction medium) provided various molecular hydrolysis products with interesting structures, such as dimeric tetraorganodistannoxanes $[R_2(X)SnOSn(Y)R_2]_2$ (**A**; X, Y = Cl, Br, OH), dimeric diorganotin hydroxy halides $[R_2Sn(OH)X]_2$ (**B**; X = Cl, Br), and trimeric diorganotin oxides *cyclo*-$(R_2SnO)_3$ (**C**) as well as polymeric diorganotin oxides, $(R_2SnO)_n$ (Chart 1).[9−25] Dimeric tetraorganodistannoxanes $[R_2(X)SnOSn(Y)R_2]_2$ (**A**; X, Y = Cl, Br, OH), possess ladder-like structures containing almost planar $Sn_4O_2X_2Y_2$ structural motifs with two pentacoordinated tin atoms incorporated in a central Sn_2O_2 four-membered ring, two pentacoordinated exocyclic tin atoms, and two bridging and two nonbridging donor groups or atoms, respectively.[16] A large number of these compounds has been investigated by X-ray diffraction studies.[21−31] Consider-

† This work contains part of the Ph.D. thesis of J.B., Dortmund University, 1999.

(1) Rochow, E. G.; Seyferth, D. *J. Am. Chem. Soc.* **1953**, *75*, 2877.
(2) Tobias, R. S.; Ogrins, I.; Nevett, B. A. *Inorg. Chem.* **1962**, *1*, 638.
(3) Nevett, B. A.; Tobias, R. S. *Chem. Ind.* **1963**, 40.
(4) Yasuda, M.; Tobias, R. S. *Inorg. Chem.* **1963**, *2*, 207.
(5) Tobias, R. S.; Yasuda, M. *Can. J. Chem.* **1964**, *42*, 781.
(6) Tobias, R. S.; Freidline, C. E. *Inorg. Chem.* **1965**, *4*, 215.
(7) Tobias, R. S.; Farrer, H. N.; Hughes, M. B.; Nevett, B. A. *Inorg. Chem.* **1966**, *5*, 2052.
(8) Arena, G.; Purrello, R.; Rizzarelli, E.; Gianguzza, A.; Pellerito, L. *J. Chem. Soc., Dalton Trans.* **1989**, 773.
(9) Cahours, A. *Liebigs Ann. Chem.* **1860**, 367.
(10) Krause, E.; Weinberg, K. *Chem. Ber.* **1930**, *63*, 381.
(11) Harada, T. *Sci. Pap. Inst. Phys. Chem. Res. (Tokyo)* **1939**, *35*, 290.
(12) Harada, T. *Rep. Sci. Res. Inst. (Japan)* **1948**, *24*, 177.
(13) Okawara, R.; Rochow, E. G. *J. Am. Chem. Soc.* **1960**, *82*, 3285.
(14) Gibbons, A. J.; Sawyer, A. K.; Ross, A. *J. Org. Chem.* **1961**, *26*, 2304.
(15) Baum, G. A.; Considine, W. J. *J. Polym. Sci.* **1963**, *B131*, 517.
(16) Okawara, R.; Wada, M. *J. Organomet. Chem.* **1963**, *1*, 81.
(17) Alleston, D. L.; Davies, A. G.; Hancock, M. *J. Chem. Soc.* **1964**, 5744.
(18) Frankel, M.; Wagner, D.; Gertner, D.; Zilkha, A. *J. Organomet. Chem.* **1967**, *9*, 83.
(19) Migdal, S.; Gertner, D.; Zilkha, A. *Can. J. Chem.* **1968**, *46*, 2409.
(20) Murray, J. D.; Chu, C. K. *J. Chem. Soc. A* **1971**, 360.
(21) Harrison, P. G.; Begley, M. J.; Molloy, K. C. *J. Organomet. Chem.* **1980**, *186*, 213.
(22) Puff, H.; Friedrichs, E.; Visel, F. *Z. Anorg. Allg. Chem.* **1981**, *477*, 50.
(23) Puff, H.; Bung, I.; Friedrichs, E.; Jansen, A. *J. Organomet. Chem.* **1983**, *254*, 23.
(24) Vollano, J. F.; Day, R. O.; Holmes, R. R. *Organometallics* **1984**, *3*, 745.
(25) Hämäläinen, R.; Turpeinen, U. *J. Organomet. Chem.* **1987**, *333*, 323.
(26) Davies, A. G. *Organotin Chemistry*; VCH: Weinheim, Germany, 1997.
(27) Graziani, R.; Casellato, U.; Plazzogna, G. *Acta Crystallogr.* **1983**, *C39*, 1188.
(28) Dakternieks, D.; Gable, R. W.; Hoskins, B. F. *Inorg. Chim. Acta* **1984**, *85*, L43.

10.1021/om010715q CCC: $22.00
Publication on Web 12/11/2001

Chart 1

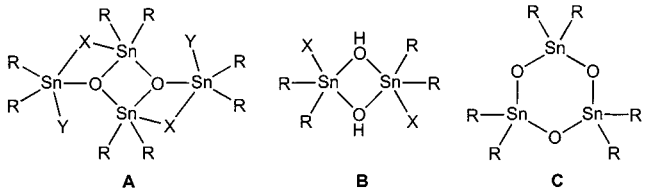

ing only two different types of donors, e.g. X, Y = Cl, OH, two symmetrically substituted dimeric tetraorganodistannoxanes, $[R_2(X)SnOSn(Y)R_2]_2$ (X = Y = Cl; X = Y = OH), and an unsymmetrically substituted dimeric tetraorganodistannoxane, (X = Cl, Y = OH), are preferably realized. In structures of the latter type, the hydroxy groups exclusively occupy the bridging positions, while the chlorine atoms are bound to the exocyclic tin atoms. This observation can be interpreted in terms of two competing donors with different donor strengths. In a recent publication, we compared structural features of all three types of dimeric tetraorganodistannoxanes, $[(t\text{-}Bu_2(X)SnOSn(Y)R_2]_2$ (X = Y = Cl; X = Cl, Y = OH; X = Y = OH; R = CH_2SiMe_3), applying the bond order concept.[30] In a continuation of this work, here we compare the molecular structures of the dimeric tetraorganodistannoxanes $[R_2(X)SnOSn(Y)R_2]_2$ (X = Y = Cl; X = Cl, Y = OH;[23] X = Y = OH; R = CH_2SiMe_3) to evaluate the influence of the organic substituents on the structural motifs. Also reported in this work is a rare example of a dimeric tetraorganodistannoxane containing fluorine atoms, $[R_2(Br)SnOSn(F)R_2]_2$ (R = CH_2SiMe_3),[32−34] which is of interest for multinuclear NMR studies. Recently, the structure and reactivity of dimeric tetraorganodistannoxanes have been studied by both solution and solid-state NMR spectroscopy.[35−38]

Only very few dimeric diorganotin hydroxy halides $[R_2Sn(OH)X]_2$ (**B**; X = F, Cl, Br, OH) have been reported so far.[39,40] In all cases investigated by X-ray diffraction, the hydroxy groups occupy the bridging positions between two pentacoordinated tin atoms, giving rise to the formation of four-membered Sn_2O_2 rings. All halides, including fluorine, are bound in exocyclic positions, demonstrating a weaker donor capacity than hydroxy groups.[41]

Trimeric diorganotin oxides *cyclo*-$(R_2SnO)_3$ (**C**) can be regarded as final products on the hydrolysis pathway of diorganotin dihalides.[42] These compounds represent six-membered Sn_3O_3 rings with tetracoordinated tin atoms in solution and the solid state. In this work we report only the second example[30] of an equilibrium between a dimeric tetraorganodistannoxane containing hydroxy groups, $[R_2(HO)SnOSn(OH)R_2]_2$, a trimeric diorganotin oxide, *cyclo*-$(R_2SnO)_3$, and water.

Despite the great number of isolated hydrolysis products from diorganotin dihalides, the hydrolysis pathway and the formation of these species is still poorly understood. In the present work we have investigated the hydrolysis of $(Me_3SiCH_2)_2SnX_2$ (X = Cl, Br) with the intention to isolate as many hydrolysis products as possible containing the same organic substituents. On the basis of these findings a general pathway for the hydrolysis of a representative diorganotin dichloride in an organic solvent with aqueous base is proposed.

Results and Discussion

The reaction of $(Me_3SiCH_2)_2SnPh_2$[43] with gaseous hydrogen chloride or bromide provided $(Me_3SiCH_2)_2SnCl_2$ (**1**) as a colorless oil and $(Me_3SiCH_2)_2SnBr_2$ (**2**) as a colorless low-melting solid, respectively, in almost quantitative yields (eq 1).

$$(Me_3SiCH_2)_2SnPh_2 + 2HX \xrightarrow[-2PhH]{} (Me_3SiCH_2)_2SnX_2 \quad (1)$$
$$X = Cl\ (\mathbf{1}),\ Br\ (\mathbf{2})$$

Both compounds have been reported before; however, no spectroscopic details were given in these reports.[44−46] In solution, $(Me_3SiCH_2)_2SnCl_2$ (**1**) and $(Me_3SiCH_2)_2SnBr_2$ (**2**) are characterized by their ^{119}Sn NMR ($CDCl_3$) chemical shifts of 146.6 and 68.3 ppm, respectively, which are indicative of tetracoordinated tin atoms. The ^{119}Sn MAS chemical shift of **2** is 77.9 ppm and differs only slightly from the respective value in solution. This unambiguously suggests that the structures in solution and in the solid state are similar.

$(Me_3SiCH_2)_2SnCl_2$ (**1**) is sensitive toward air moisture and reacts with water to give the adduct $(Me_3SiCH_2)_2SnCl_2{\cdot}H_2O$ (**1a**) as a low-melting solid in quantitative yield (eq 2).[47]

$$\underset{\mathbf{1}}{(Me_3SiCH_2)_2SnCl_2} + H_2O \xrightarrow{CDCl_3} \underset{\mathbf{1a}}{(Me_3SiCH_2)_2SnCl_2{\cdot}H_2O} \quad (2)$$

The molecular structure of **1a** is shown in Figure 1; crystallographic data are given in Table 1, and selected bond lengths and angles are listed in Table 2. At first approximation, the tin atom in **1a** shows a distorted-

(29) Reuter, H.; Pawlak, R. *Acta Crystallogr.* **2000**, *C56*, 804.
(30) Beckmann, J.; Jurkschat, K.; Rabe, S.; Schürmann, M.; Dakternieks, D. *Z. Anorg. Allg. Chem.* **2001**, *627*, 458.
(31) Janzen, M. C.; Jennings, M. C.; Puddephatt, R. J. *Organometallics* **2001**, *20*, 4100.
(32) Jain, V. K.; Mokal, V. B.; Sandor, P. *Magn. Reson. Chem.* **1992**, *30*, 1158.
(33) Beckmann, J.; Biesemans, M.; Hassler, K.; Jurkschat, K.; Martins, J. C.; Schürmann, M.; Willem, R. *Inorg. Chem.* **1998**, *37*, 4891.
(34) Dakternieks, D.; Kuan, F. S.; Tiekink, E. R. T. 10th International Conference on the Coordination and Organometallic Chemistry of Germanium, Tin, and Lead, Bordeaux, France, 2001; Book of Abstracts 2P5.
(35) Gross, D. C. *Inorg. Chem.* **1989**, *28*, 2355.
(36) Ribot, F.; Sanchez, C.; Meddour, A.; Gielen, M.; Tiekink, E. R. T.; Biesemans, M.; Willem, R. *J. Organomet. Chem.* **1998**, *552*, 177.
(37) Hasha, D. L. *J. Organomet. Chem.* **2001**, *620*, 296.
(38) Tierney, D. L.; Moehs, P. J.; Hasha, D. L. *J. Organomet. Chem.* **2001**, *620*, 211.
(39) Puff, H.; Hevendehl, H.; Höfer, K.; Reuter, H.; Schuh, W. *J. Organomet. Chem.* **1985**, *287*, 163.
(40) Beckmann, J.; Jurkschat, K.; Mahieu, B.; Schürmann, M. *Main Group Met. Chem.* **1998**, *21*, 113.
(41) Beckmann, J.; Mahieu, B.; Nigge, W.; Schollmeyer, D.; Schürmann, M.; Jurkschat, K. *Organometallics* **1998**, *17*, 5697.
(42) Beckmann, J.; Jurkschat, K.; Rabe, S.; Schürmann, M. *Z. Anorg. Allg. Chem.*, in press.
(43) Kong, X.; Grindley, T. B.; Bakshi, P. K.; Cameron, T. S. *Organometallics* **1993**, *12*, 4881.
(44) Seyferth, D. *J. Am. Chem. Soc.* **1957**, *79*, 5881.
(45) Mironov, V. F.; Stepina, E. M.; Shiryaev, V. I. *Zh. Obshch. Khim.* **1972**, *42*, 631.
(46) Glocking, F.; Sweeney, J. J. *J. Chem. Res., Miniprint* **1977**, 612.
(47) Belsky, V. K.; Zemlyanskii, N. N.; Kolosova, N. D.; Borisova, I. V. *J. Organomet. Chem.* **1981**, *215*, 41.

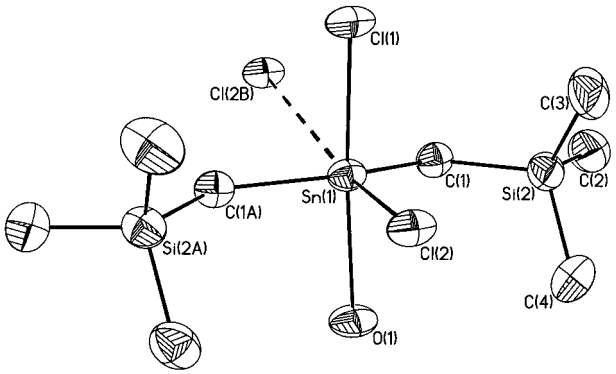

Figure 1. General view (SHELXTL-PLUS) of a molecule of **1a** showing 30% probability displacement ellipsoids and the atom numbering, Symmetry transformations used to generate equivalent atoms: (a) $x, -y, z$; (b) $x, y, z + 1$.

trigonal-bipyramidal configuration (geometrical goodness $\Delta(\Sigma\vartheta) = 73.7°$)[48,49] with C(1), C(1a), and Cl(2) occupying the equatorial positions and Cl(1) and O(1) occupying the axial positions. The tin atom is displaced by 0.192(5) Å in the direction of Cl(1). The Sn(1)−Cl(1), Sn(1)−Cl(2), and Sn(1)−O(1) bond lengths amount to 2.497(3), 2.376(2), and 2.405(8) Å, respectively, and are comparable to those of other water adducts of organotin chlorides.[50] The distortion of the trigonal-bipyramidal geometry is documented best in the O(1)−Sn(1)−C(1) and C(1)−Sn(1)−C(1a) angles, being 171.0(2) and 133.5(3)°. The widening of the latter angle is caused by a weakly coordinating (edge-attacking)[51] chlorine atom (Sn(1)···Cl(2b) = 3.805(2) Å) from a neighbor molecule giving rise to the formation of a one-dimensional infinite chain in the solid state with an overall [5 + 1] coordination at tin. The hypercoordination in **1a** is also reflected in the ^{119}Sn MAS chemical shift of −53.9 ppm. Upon dissolution in $CDCl_3$ the water adduct $(Me_3SiCH_2)_2SnCl_2 \cdot H_2O$ (**1a**) undergoes complete dissociation, as is shown by ^{119}Sn NMR spectroscopy exhibiting exclusively the chemical shift of the parent $(Me_3SiCH_2)_2SnCl_2$ (**1**) mentioned before (eq 2). In contrast to the diorganotin dichloride **1**, the corresponding dibromide $(Me_3SiCH_2)_2SnBr_2$ (**2**) forms no such water adduct.

The reaction of $(Me_3SiCH_2)_2SnCl_2$ (**1**) with water in the presence of appropriate amounts of triethylamine afforded the dimeric tetraorganodistannoxane $[R_2(Cl)SnOSn(Cl)R_2]_2$ (**3**; R = CH_2SiMe_3) as a colorless high-melting solid in good yield (eq 3).

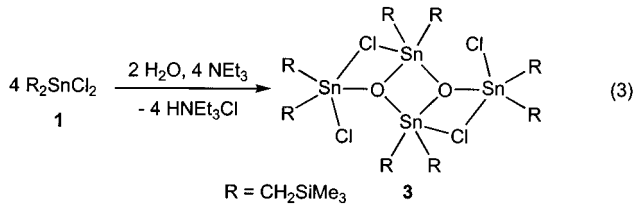

The ^{119}Sn NMR spectrum of **3** ($CDCl_3$) reveals two equally intense signals at −60.1 ppm ($^2J(^{119}Sn-O-^{117/119}Sn)$ = 73 Hz) and −133.5 ppm ($^2J(^{119}Sn-O-^{117/119}Sn)$ = 77 Hz). The ^{119}Sn MAS NMR spectrum shows four signals at −28.4, −54.6, −124.0, and −131.6 ppm, which are in good agreement with the ^{119}Sn NMR chemical shifts found in solution. The number of signals confirms the absence of a crystallographic center of inversion for the molecular structure of **3** as determined by single-crystal X-ray diffraction. The molecular structure of $[R_2(Cl)SnOSn(Cl)R_2]_2$ (**3**; R = CH_2SiMe_3) is shown in Figure 2; crystallographic data are given in Table 1, and selected bond lengths and angles are listed in Table 3. A discussion of the molecular structure is given below.

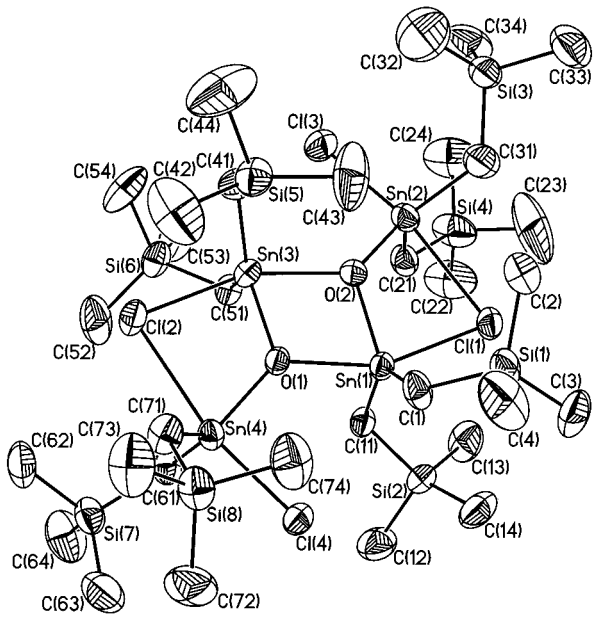

Figure 2. General view (SHELXTL-PLUS) of a molecule of **3** showing 30% probability displacement ellipsoids and the atom numbering.

The hydrolysis of $(Me_3SiCH_2)_2SnBr_2$ (**2**) with stoichiometric amounts of sodium hydroxide provided the dimeric tetraorganodistannoxane $[R_2(Br)SnOSn(OH)R_2]_2$ (**4**; R = CH_2SiMe_3) as a colorless high-melting solid in good yield (Scheme 1).

The ^{119}Sn NMR spectrum of **4** ($CDCl_3$) reveals two equally intense signals at −155.2 ppm ($\nu_{1/2}$ = 50 Hz, $^2J(^{119}Sn-O-^{117/119}Sn)$ = 210 Hz) and −171.2 ppm ($\nu_{1/2}$ = 15 Hz, $^2J(^{119}Sn-O-^{117/119}Sn)$ = 213 Hz). The ^{119}Sn MAS NMR spectrum of **4** shows four signals at −159.6, −169.5, −176.9, and −186.4 ppm, which suggests that the solid-state modification possesses no centrosymmetry. No attempts were made to determine the molecular structure of **4**.

Repeating the latter reaction in the presence of stoichiometric amounts of sodium fluoride afforded the fluorine-containing dimeric tetraorganodistannoxane $[R_2(Br)SnOSn(F)R_2]_2$ (**5**; R = CH_2SiMe_3) as a high-melting solid in good yield (Scheme 1). The preference of fluorine atoms over hydroxy groups in the formation of **5** is unexpected and is in marked contrast to the established order of donor strength $OH^- > F^-$.[39] The ^{119}Sn NMR spectrum of **5** ($CDCl_3$) shows two equally intense signals at −118.4 ppm ($^1J(^{119}Sn-^{19}F)$ = 988 Hz; $^2J(^{119}Sn-O-^{117/119}Sn)$ = 196 Hz) and −131.3 ppm ($^1J(^{119}Sn-^{19}F)$ = 1560 Hz; $^2J(^{119}Sn-O-^{117/119}Sn)$ = 203 Hz; $^3J(^{119}Sn-O-^{19}F)$ = 30 Hz) with a total integral of

(48) Kolb, U.; Beuter, M.; Dräger, M. *Inorg. Chem.* **1994**, *33*, 4522.
(49) Beuter, M.; Kolb, U.; Zickgraf, A.; Bräu, E.; Bletz, M.; Dräger, M. *Polyhedron* **1997**, *16*, 4005.
(50) Johnson, S. E.; Knobler, C. B. *Organometallics* **1994**, *13*, 4928.
(51) Jastrzebski, J. T. B. H.; van der Schaaf, P. A.; Boersma, J.; van Koten, G.; de Ridder, D. J. A.; Heijdenreijk, D. *Organometallics* **1992**, *11*, 1521.

Table 1. Crystallographic Data for 1a, 3, 6, and 7

	1a	3	6	7
formula	$C_8H_{22}Cl_2Si_2Sn\cdot H_2O$	$C_{32}H_{88}Cl_4O_2Si_8Sn_4$	$C_{32}H_{92}O_6Si_8Sn_4$	$C_{24}H_{66}O_3Si_6Sn_3$
fw	382.04	1346.30	1272.54	927.38
cryst syst	monoclinic	triclinic	triclinic	triclinic
cryst size, mm	0.1 × 0.1 × 0.08	0.2 × 0.15 × 0.15	0.2 × 0.18 × 0.18	0.2 × 0.15 × 0.15
space group	*Cm*	$P\bar{1}$	$P\bar{1}$	$P\bar{1}$
a, Å	7.053(1)	12.647(1)	12.507(1)	12.249(1)
b, Å	23.787(1)	15.243(1)	12.563(1)	12.425(1)
c, Å	6.160(1)	17.761(1)	12.616(1)	16.151(1)
α, deg	90	83.006(1)	68.851(1)	102.925(1)
β, deg	123.425(1)	80.357(1)	62.143(1)	90.866(1)
γ, deg	90	68.730(1)	63.135(1)	109.173(1)
V, Å^3	862.5(2)	3138.7(4)	1535.0(2)	2252.4(3)
Z	2	2	1	2
ρ_{calcd}, Mg/m^3	1.471	1.425	1.377	1.367
ρ_{meas}, Mg/m^3	1.457(4)	1.414(2)	n.m.	n.m.
μ, mm^{-1}	1.907	1.919	1.794	1.830
F(000)	384	1352	644	936
θ range, deg	4.31 to 25.70	4.11 to 25.68	3.45 to 25.42	4.09 to 25.33
index ranges	$-8 \le h \le 8$	$-15 \le h \le 15$	$-15 \le h \le 15$	$-13 \le h \le 13$
	$-28 \le k \le 28$	$-16 \le k \le 18$	$-13 \le k \le 15$	$-14 \le k \le 13$
	$-6 \le l \le 6$	$-18 \le l \le 19$	$-12 \le l \le 18$	$-19 \le l \le 19$
no. of rflns collcd	4920	42 453	20 259	29 107
completeness to θ_{max}, %	92.1	92.3	92.1	91.6
no. of indep rflns/R_{int}	1519/0.041	11018/0.067	5212/0.046	7536/0.052
no. of rflns obsd with $I > 2\sigma(I)$	1458	7256	2633	5090
no. of refined params	74	488	235	344
GOF(F^2)	1.094	0.980	0.907	0.920
R1(F) ($I > 2\sigma(I)$)	0.0326	0.0461	0.0454	0.0301
wR2(F^2) (all data)	0.0802	0.1185	0.0928	0.0633
$(\Delta/\sigma)_{max}$	<0.001	<0.001	<0.001	<0.001
largest diff peak/hole, e/Å^3	0.326/−0.750	1.086/−0.954	0.890/−0.516	0.353/−0.486

Table 2. Selected Bond Lengths (Å) and Angles (deg) for 1a[a]

Sn(1)−O(1)	2.404(8)	Sn(1)−Cl(1)	2.497(3)
Sn(1)−Cl(2)	2.375(2)	Sn(1)−Cl(2b)	3.805(2)
Sn(1)−C(1)	2.109(7)		
O(1)−Sn(1)−Cl(1)	171.0(2)	O(1)−Sn(1)−Cl(2)	81.1(2)
Cl(1)−Sn(1)−Cl(2)	89.82(9)	O(1)−Sn(1)−C(1)	86.5(2)
Cl(1)−Sn(1)−C(1)	97.0(2)	Cl(2)−Sn(1)−C(1)	112.1(2)
C(1)−Sn(1)−C(1a)	133.5(3)		

[a] Symmetry transformations used to generate equivalent atoms: (a) *x*, −*y*, *z*; (b) *x*, *y*, *z* + 1.

Table 3. Selected Bond Lengths (Å) and Angles (deg) for 3

Sn(1)−O(1)	2.203(3)	Sn(1)−O(2)	2.054(3)
Sn(1)−Cl(1)	2.5775(15)	Sn(1)−Cl(4)	3.6477(17)
Sn(1)−C(1)	2.108(6)	Sn(1)−C(11)	2.119(5)
Sn(2)−O(2)	2.021(3)	Sn(2)−Cl(1)	2.9206(16)
Sn(2)−Cl(3)	2.3949(18)	Sn(2)−C(21)	2.117(6)
Sn(2)−C(31)	2.148(7)	Sn(3)−O(1)	2.051(3)
Sn(3)−O(2)	2.191(3)	Sn(3)−Cl(2)	2.5865(16)
Sn(3)−Cl(3)	3.6161(19)	Sn(3)−C(41)	2.126(6)
Sn(3)−C(51)	2.123(5)	Sn(4)−O(1)	2.015(3)
Sn(4)−Cl(2)	2.8574(16)	Sn(4)−Cl(4)	2.4137(16)
Sn(4)−C(61)	2.131(6)	Sn(4)−C(71)	2.129(5)
O(1)−Sn(1)−O(2)	74.78(13)	O(1)−Sn(1)−Cl(1)	156.37(10)
O(1)−Sn(1)−C(1)	93.23(19)	O(1)−Sn(1)−C(11)	94.66(17)
O(2)−Sn(1)−Cl(1)	81.61(10)	O(2)−Sn(1)−C(1)	118.9(2)
O(2)−Sn(1)−C(11)	107.96(18)	C(11)−Sn(1)−Cl(1)	93.41(16)
C(1)−Sn(1)−Cl(1)	97.44(17)	C(1)−Sn(1)−C(11)	132.9(3)
O(2)−Sn(2)−Cl(1)	73.77(10)	O(2)−Sn(2)−Cl(3)	93.19(11)
O(2)−Sn(2)−C(21)	108.8(2)	O(2)−Sn(2)−C(31)	114.3(2)
Cl(3)−Sn(2)−Cl(1)	166.91(6)	Cl(1)−Sn(2)−C(21)	85.06(19)
Cl(1)−Sn(2)−C(31)	81.65(19)	Cl(3)−Sn(2)−C(21)	98.42(19)
Cl(3)−Sn(2)−C(31)	105.4(2)	C(21)−Sn(2)−C(31)	128.7(3)
O(1)−Sn(3)−O(2)	75.08(13)	O(1)−Sn(3)−Cl(2)	80.79(10)
O(1)−Sn(3)−C(41)	122.0(2)	O(1)−Sn(3)−C(51)	107.85(18)
O(2)−Sn(3)−Cl(2)	155.71(10)	O(2)−Sn(3)−C(41)	98.5(2)
O(2)−Sn(3)−C(51)	95.92(17)	Cl(2)−Sn(3)−C(41)	91.8(2)
Cl(2)−Sn(3)−C(51)	94.07(16)	C(41)−Sn(3)−C(51)	130.1(2)
O(1)−Sn(4)−Cl(2)	74.78(10)	O(1)−Sn(4)−Cl(4)	92.52(10)
O(1)−Sn(4)−C(61)	112.0(2)	O(1)−Sn(4)−C(71)	114.5(2)
Cl(2)−Sn(4)−Cl(4)	167.14(5)	Cl(2)−Sn(4)−C(61)	85.51(18)
Cl(2)−Sn(4)−C(71)	83.50(18)	Cl(4)−Sn(4)−C(61)	97.69(17)
Cl(4)−Sn(4)−C(71)	104.04(18)	C(61)−Sn(4)−C(71)	127.1(3)
Sn(1)−O(1)−Sn(3)	104.11(14)	Sn(1)−O(1)−Sn(4)	130.44(16)
Sn(3)−O(1)−Sn(4)	121.30(16)	Sn(1)−O(2)−Sn(2)	121.74(17)
Sn(1)−O(2)−Sn(3)	104.45(15)	Sn(2)−O(2)−Sn(3)	128.34(17)
Sn(1)−Cl(1)−Sn(2)	80.44(4)	Sn(3)−Cl(2)−Sn(4)	81.07(4)
Sn(2)−Cl(3)−Sn(3)	75.19(5)	Sn(1)−Cl(4)−Sn(4)	75.32(4)

90% (Figure 3). Furthermore, there are nine additional low-intensity signals at −111.2, −116.2, −117.4, −120.2, −123.3, −128.3, −130.0, −131.0, and −136.8 ppm (indicated by arrows in Figure 3) with a total integral of 10%, which were not assigned. However, the fact that these signals are reproducible with the same integral ratio for solutions of samples which had been recrystallized several times suggests the species belonging to these signals are in equilibrium with compound **5**.

The ^{19}F NMR spectrum of **5** reveals one major signal at −78.9 ppm ($^1J(^{19}F-^{119}Sn)$ = 1554 Hz; $^1J(^{19}F-^{117/119}Sn)$ = 976 Hz; in Figure 4 denoted with "M") with a total integral of 90% and three low-intensity signals at −74.9 ppm ($^1J(^{19}F-^{119}Sn)$ = 1557 Hz; $^1J(^{19}F-^{117/119}Sn)$ = 1045 Hz; $^4J(^{19}F-^{19}F)$ = 43 Hz; in Figure 4 denoted with "m1"), −79.2 ppm ($^1J(^{19}F-^{119}Sn)$ = 1617 Hz; $^1J(^{19}F-^{117/119}Sn)$ = 912 Hz; in Figure 4 denoted with "m2"), and −138.2 ppm ($^1J(^{19}F-^{119}Sn)$ = 2517 Hz; $^4J(^{19}F-^{19}F)$ = 47 Hz; in Figure 4 denoted with "m3") with a total integral of 10%, for which no assignment was made.

The ^{119}Sn MAS NMR spectrum of **5** shows two signals at −110.3 ppm ($^1J(^{119}Sn-^{19}F)$ = 854 Hz) and −156.8 ppm ($^1J(^{119}Sn-^{19}F)$ = 1617 Hz). The number of signals suggests the existence of a crystallographic center of inversion in the solid-state modification of **5**. Attempts to grow single crystals suitable for an X-ray structure analysis failed, and only twinned crystals were obtained.

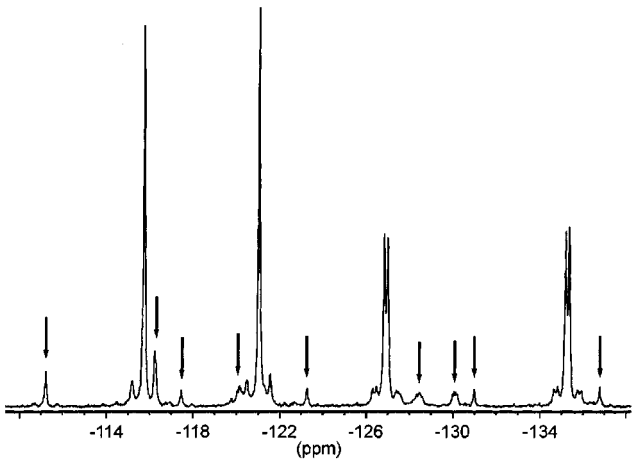

Figure 3. ^{119}Sn NMR spectrum (400.21 MHz, $CDCl_3$) of $[R_2(Br)SnOSn(F)R_2]_2$ (**5**; R = CH_2SiMe_3). Low-intensity signals systematically related to **5** are indicated by arrows.

Scheme 1

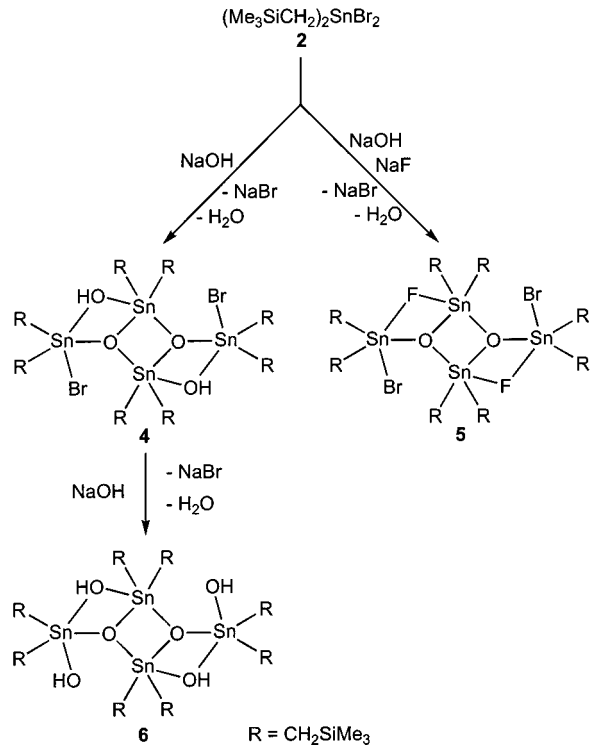

According to ^{119}Sn NMR studies, the hydrolysis of $(Me_3SiCH_2)_2SnCl_2$ (**1**) with sodium hydroxide in the presence of sodium fluoride appeared to give mixtures of different species. All attempts to separate these species failed.

Further hydrolysis of $[R_2(Br)SnOSn(OH)R_2]_2$ (**4**; R = CH_2SiMe_3) with an excess of sodium hydroxide provided the dimeric tetraorganodistannoxane $[R_2(HO)SnOSn(OH)R_2]_2$ (**6**; R = CH_2SiMe_3) as a colorless high-melting solid in reasonable yield (Scheme 1). The ^{119}Sn NMR spectrum of **6** ($CDCl_3$) shows two equally intense major signals at −142.2 ppm ($\nu_{1/2}$ = 400 Hz) and −162.6 ppm ($\nu_{1/2}$ = 400 Hz) with a total integral of 80% belonging to the two pentacoordinated tin atoms of **6** and a lower intense signal at 48.2 ppm (integral 20%), which is assigned to *cyclo*-$[(Me_3SiCH_2)_2SnO]_3$ (**7**) (see below). The ^{119}Sn MAS NMR of **6** shows two signals at −143.8 and −162.6 ppm, which is consistent with the centrosymmetric space group found in the single-crystal X-ray structure analysis and which reveals the structures in solution and in the solid state to be similar. The molecular structure of $[R_2(HO)SnOSn(OH)R_2]_2$ (**6**; R = CH_2SiMe_3) is shown in Figure 5; crystallographic data are given in Table 1, and selected bond lengths and angles are listed in Table 4. A discussion of the molecular structure is given below.

Table 4. Selected Bond Lengths (Å) and Angles (deg) for 6[a]

Sn(1)−O(1)	2.147(4)	Sn(1)−O(2)	2.047(4)
Sn(1)−O(2a)	2.129(4)	Sn(1)−O(3a)	3.583(5)
Sn(1)−C(1)	2.109(6)	Sn(1)−C(11)	2.134(7)
Sn(2)−O(1)	2.342(4)	Sn(2)−O(2)	2.019(4)
Sn(2)−O(3)	2.032(4)	Sn(2)−C(21)	2.111(6)
Sn(2)−C(31)	2.128(7)		
O(2)−Sn(1)−O(1)	74.27(15)	O(1)−Sn(1)−O(2a)	146.59(15)
O(2)−Sn(1)−O(2a)	72.50(17)	O(1)−Sn(1)−C(1)	95.2(2)
O(1)−Sn(1)−C(11)	100.6(2)	O(2)−Sn(1)−C(1)	119.5(2)
O(2)−Sn(1)−C(11)	120.8(2)	O(2a)−Sn(1)−C(1)	98.1(2)
O(2a)−Sn(1)−C(11)	99.1(2)	C(1)−Sn(1)−C(11)	119.7(3)
O(1)−Sn(2)−O(2)	70.57(14)	O(1)−Sn(2)−O(3)	158.49(18)
O(2)−Sn(2)−O(3)	88.67(17)	O(1)−Sn(2)−C(21)	87.3(2)
O(1)−Sn(2)−C(31)	93.2(2)	O(2)−Sn(2)−C(21)	118.1(2)
O(2)−Sn(2)−C(31)	110.8(3)	O(3)−Sn(2)−C(21)	98.0(2)
O(3)−Sn(2)−C(31)	99.6(3)	C(21)−Sn(2)−C(31)	128.0(3)
Sn(1)−O(2)−Sn(1a)	107.50(17)	Sn(1)−O(1)−Sn(2)	99.62(15)
Sn(1)−O(2)−Sn(2)	115.12(16)	Sn(1a)−O(2)−Sn(2)	136.47(19)

[a] Symmetry transformations used to generate equivalent atoms: (a) $-x, -y, -z - 1$.

In solution the dimeric tetraorganodistannoxane $[R_2(HO)SnOSn(OH)R_2]_2$ (**6**; R = CH_2SiMe_3) is in equilibrium with *cyclo*-$[(Me_3SiCH_2)_2SnO]_3$ (**7**) and water (eq 4).

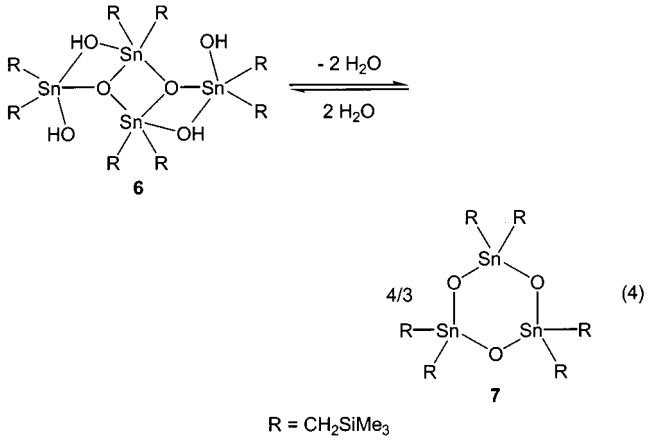

(4)

Heating a solution of **6** in toluene in a Dean−Stark apparatus for a short time in order to remove the water indeed shifted the equilibrium toward *cyclo*-$[(Me_3SiCH_2)_2SnO]_3$ (**7**). However, the water could not be removed completely by applying this method, even after prolonged heating. Complete removal of water was accomplished by adding activated molecular sieves to the aforementioned solution, providing *cyclo*-$[(Me_3SiCH_2)_2SnO]_3$ (**7**) as a colorless low-melting solid (eq 4). The synthesis of *cyclo*-$[(Me_3SiCH_2)_2SnO]_3$ (**7**) was claimed in a previous report;[43] however, the previously reported melting point of 152 °C is very close to that found for $[R_2(HO)SnOSn(OH)R_2]_2$ (**6**; R = CH_2SiMe_3) in this work. Moreover, in an early report the final hydrolysis product of $(Me_3SiCH_2)_2SnCl_2$ (**1**) was assumed to be polymeric $[(Me_3SiCH_2)_2SnO]_n$, but at that time no spectroscopic

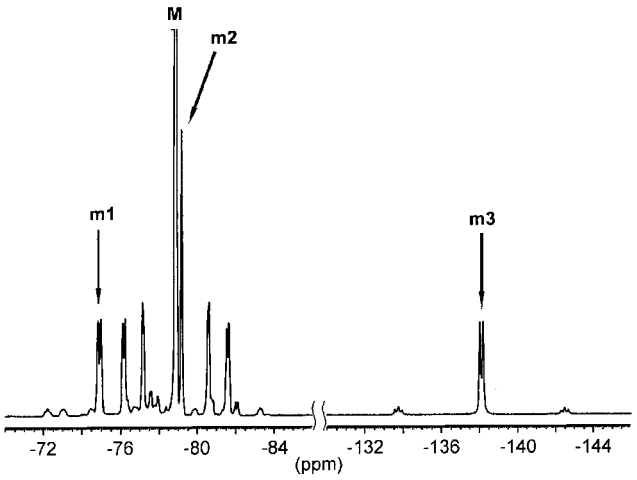

Figure 4. ^{19}F NMR spectrum (282.40 MHz, $CDCl_3$) of $[R_2(Br)SnOSn(F)R_2]_2$ (**5**; R = CH_2SiMe_3). The major signal (M) and the systematically related low-intensity signals (m1−m3) are indicated by arrows.

details were available to support this assumption.[44] The ^{119}Sn NMR spectrum (toluene-d_8, c = 0.323 mol/L) of an analytically pure sample of *cyclo*-$[(Me_3SiCH_2)_2SnO]_3$ (**7**) is temperature-dependent and shows a major resonance **a** (T = 23 °C, δ 49.6, $\nu_{1/2}$ = 112 Hz, integral 86; T = −40 °C, δ 52.9, $\nu_{1/2}$ = 14 Hz, $^2J(^{119}Sn-O-^{117}Sn)$ = 346 Hz, integral 75) and minor resonances **b** (T = 23 °C, δ 36.9, $\nu_{1/2}$ = 66 Hz, integral 8; T = −40 °C, δ 47.5, $\nu_{1/2}$ = 21 Hz, $^2J(^{119}Sn-O-^{117}Sn)$ = 437 Hz, integral 20), **c** (T = 23 °C, δ −134.0, $\nu_{1/2}$ = 72 Hz, integral 3; T = −40 °C, δ −135.1, $\nu_{1/2}$ = 51 Hz, integral 2.5), and **d** (T = 23 °C, δ −155.5, $\nu_{1/2}$ = 65 Hz, integral 3; T = −40 °C, δ −153.5, $\nu_{1/2}$ = 34 Hz, integral 2.5). Signal **a** belongs to *cyclo*-$[(Me_3SiCH_2)_2SnO]_3$ (**7**), whereas signals **c** and **d** are assigned to the tetraorganodistannoxane **6**. Signal **b** is assigned with caution to the eight-membered-ring *cyclo*-$[(Me_3SiCH_2)_2SnO]_4$ (**7a**) or a higher oligomer in equilibrium with **7**. Arguments in favor of the assignment of signal **b** are (i) the satellite-to-signal integral ratio of 8:84:8 and (ii) the chemical shift being slightly low-frequency shifted with respect to the six-membered ring *cyclo*-$[(Me_3SiCH_2)_2SnO]_3$ (**7**) but still being in the region for tetracoordinated diorganotin compounds. From systematic studies on *cyclo*-stannasiloxanes it is known that the chemical shift depends on the ring size.[41] The ^{119}Sn MAS NMR spectrum of **7** shows three signals at 68.5 ppm ($^2J(^{119}Sn-O-^{117/119}Sn)$ = 299 Hz), 49.5 ppm ($^2J(^{119}Sn-O-^{117/119}Sn)$ = 281 Hz), and 46.6 ppm ($^2J(^{119}Sn-O-^{117/119}Sn)$ = 274 Hz), which are close to the chemical shift found in solution. The number of signals is consistent with the number of crystallographically independent tin sites present in the solid-state structure of **7** (Figure 6).

The molecular structure of *cyclo*-$[(Me_3SiCH_2)_2SnO]_3$ (**7**) is shown in Figure 7; crystallographic data are given in Table 1, and selected bond lengths and angles are listed in Table 5.

All tin atoms show distorted-tetrahedral geometries, with the distortion being manifested in the average C−Sn−C and O−Sn−O angles of 118.3(2) and 103.2(2)°, respectively. The mean Sn−O and Sn−C bond lengths of 1.955(3) and 2.130(4) Å resemble those of other diorganotin oxides.[42] The most striking feature of

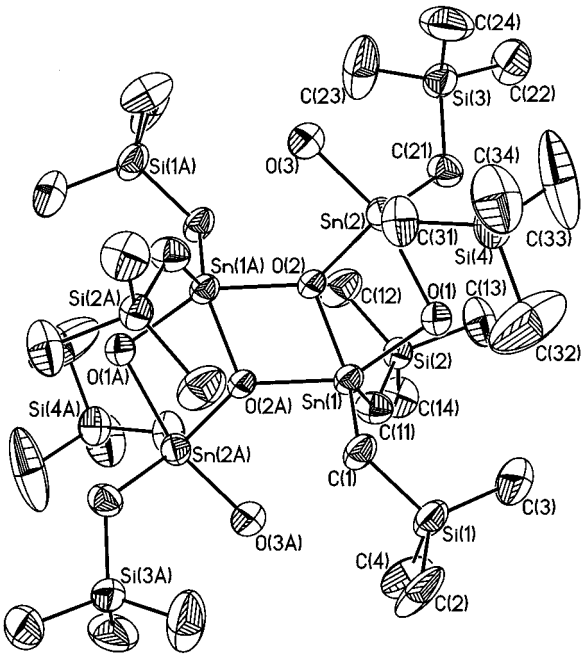

Figure 5. General view (SHELXTL-PLUS) of a molecule of **6** showing 30% probability displacement ellipsoids and the atom numbering. Symmetry transformations used to generate equivalent atoms: (a) $-x, -y, -z - 1$.

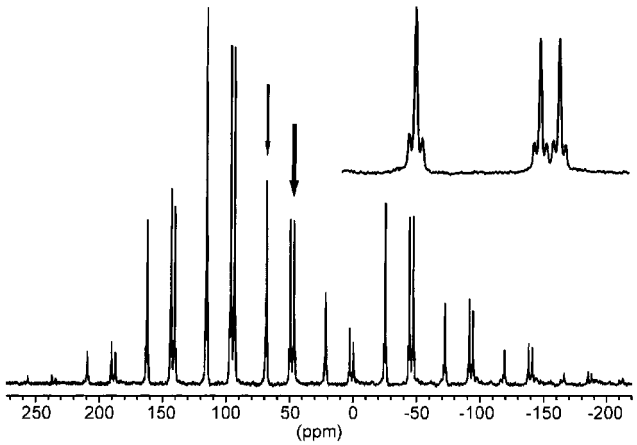

Figure 6. ^{119}Sn MAS NMR spectrum (400.21 MHz, spinning rate 6 kHz, 10 K transients) of *cyclo*-$[(Me_3SiCH_2)_2SnO]_3$ (**7**). The three center bands are indicated by arrows and depicted in the enlargement.

the molecular structure of **7** is the highly puckered conformation of the Sn_3O_3 ring, which is in contrast to the more or less planar ring conformations found for other trimeric diorganotin oxides.[42] It is of note that the related *cyclo*-$[(Me_3SiCH_2)_2SnTe]_3$ reveals also a strongly puckered ring conformation, which can tentatively be traced to crystal packing effects.[52a] The average Sn−O−Sn angle of 122.4(1)° is substantially smaller than in other diorganotin oxides and likely to be of the same origin. The highly puckered ring conformation is also reflected in the sum of internal ring angles being 676.9°, which differs significantly from 720°, the sum associated with a perfectly planar six-membered ring.

(52) (a) Einstein, F. W. B.; Gay, I. D.; Jones, C. H. W.; Riesen, A.; Sharma, R. D. *Acta Crystallogr.* **1993**, *C49*, 470. (b) Huheey, J.; Keiter, E. A.; Keiter, R. L. *Inorganic Chemistry: Principles of Structure and Reactivity*, 2nd ed.; de Gruyter: New York, Berlin 1995.

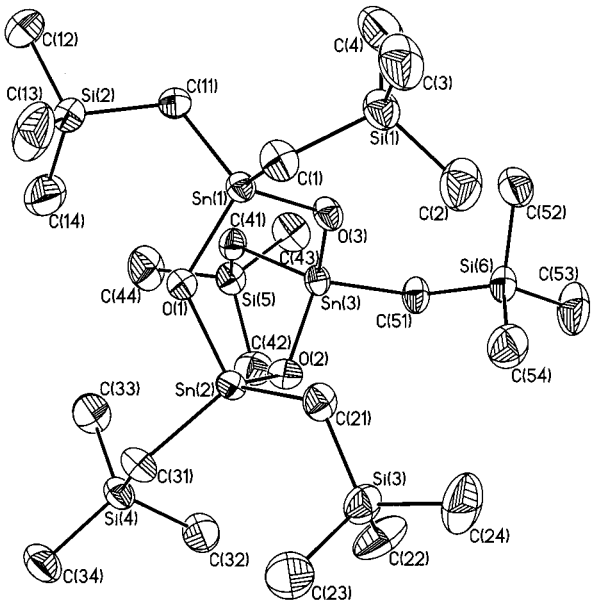

Figure 7. General view (SHELXTL-PLUS) of a molecule of **7** showing 30% probability displacement ellipsoids and the atom numbering.

The hydrolysis of $(Me_3SiCH_2)_2SnCl_2$ (**1**) with sodium hydroxide was reported to give the dimeric tetraorganodistannoxane $[R_2(Cl)SnOSn(OH)R_2]_2$ (**8**; R = CH_2SiMe_3).[23] Compound **8** was previously investigated by single-crystal X-ray diffraction, but no ^{119}Sn NMR parameters were reported.[23] An alternative approach for the almost quantitative synthesis of $[R_2(Cl)SnOSn(OH)R_2]_2$ (**8**; R = CH_2SiMe_3) is the redistribution reaction between $[R_2(Cl)SnOSn(Cl)R_2]_2$ (**3**; R = CH_2SiMe_3) and $[R_2(HO)SnOSn(OH)R_2]_2$ (**6**; R = CH_2SiMe_3) (eq 5).

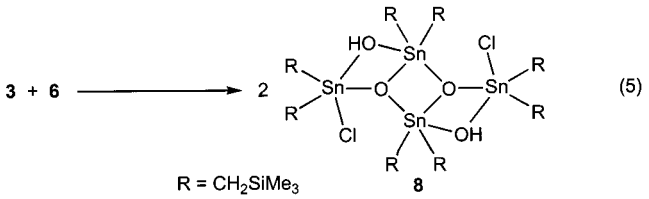

The ^{119}Sn NMR spectrum ($CDCl_3$) of **8** shows two equally intense signals at −147.0 ppm ($\nu_{1/2}$ = 25 Hz, $^2J(^{119}Sn-O-^{117}Sn)$ = 215 Hz) and −153.9 ppm ($\nu_{1/2}$ = 50 Hz, $^2J(^{119}Sn-O-^{117}Sn)$ = 220 Hz). The ^{119}Sn MAS NMR spectrum of **8** shows more than four signals in the range between −72 and −176 ppm; however, as a result of overlapping with spinning sidebands we failed to unambiguously determine the isotropic chemical shifts. We tentatively attribute the high number of signals to the presence of different crystal modifications in the bulk material.

Molecular Structures of the Dimeric Tetraorganodistannoxanes 3, 6, and 8. The symmetrically substituted dimeric tetraorganodistannoxanes $[R_2(X)SnOSn(X)R_2]_2$ (**3**, X = Cl; **6**, X = OH; R = CH_2SiMe_3) crystallize in the *triclinic* space group $P\bar{1}$, while for the unsymmetrically substituted analogue $[R_2(Cl)SnOSn(OH)R_2]_2$ (**8**; R = CH_2SiMe_3) the *orthorhombic* space group $Pna2_1$ was reported.[23] Notably, the related dimeric tetraorganodistannoxanes $[t\text{-}Bu_2(X)SnOSn(Y)R_2]_2$ (X = Y = Cl; X = Cl, Y = OH; X = Y = OH; R = CH_2SiMe_3) all crystallize in the *monoclinic* space group *C*2/*c*.[30] Apparently, this observation suggests that the organic substituents of the exocyclic tin atoms, e.g. CH_2SiMe_3 and *t*-Bu groups, have a significant influence on the preferred modification in the solid state. Among the dimeric tetraorganodistannoxanes described in this work, only $[R_2(HO)SnOSn(OH)R_2]_2$ (**6**; R = CH_2SiMe_3) reveals a crystallographic center of inversion at 0.0, 0.0, and −0.5. In agreement with all other molecular structures of dimeric tetraorganodistannoxanes two tin atoms of $[R_2(X)SnOSn(Y)R_2]_2$ (**3**, X = Y = Cl; **6**, X = Y = OH; **8**,[23] X = Cl, Y = OH; R = CH_2SiMe_3) are incorporated in a central Sn_2O_2 four-membered ring (Sn(1) and Sn(3) for **3**, Sn(1) and Sn(1a) for **6**, Sn(1) and Sn(2) for **8**[23]) and two tin atoms (Sn(2) and Sn(4) for **3**, Sn(2) and Sn(2a) for **6**, Sn(3) and Sn(4) for **8**) are located exocyclic to these rings. The $Sn_4O_2X_4$ structural motifs are planar to a deviation of fitted atoms of ±0.180 Å in **3**, to ±0.062 Å in **6**, and to ±0.086 Å in **8**.[23] Each tin atom reveals a distorted-trigonal-bipyramidal geometry, with the equatorial positions being occupied by two carbons and one oxygen (C(1), C(11), O(2) for Sn(1), C(21), C(31), O(2) for Sn(2), C(41), C(51), O(1) for Sn(3), and C(61), C(71), O(1) for Sn(4) in **3**; C(1), C(11), O(2) for Sn(1) and C(21), C(31), O(2) for Sn(2) in **6**; C(10), C(50), O(1) for Sn(1), C(20), C(60), O(2) for Sn(2), C(30), C(70), O(1) for Sn(3), and C(40), C(80), O(2) for Sn(4) in **8**[23]). The axial positions are occupied by an oxygen atom (O(1) for Sn(1) and O(2) for Sn(3) in **3**; O(2a) in **6**; O(2) for Sn(1) in **8**[23]) and by one donor atom X (X = Cl(1) for Sn(1) and X = Cl(2) for Sn(3) in **3**; X = O(1) for Sn(1) in **6**; X = O(3) for Sn(1) and X = O(4) for Sn(2) in **8**[23]) in the case of the endocyclic tin atoms and by two donor atoms X and Y (X = Cl(1), Y = Cl(3) for Sn(2) and X = Cl(2), Y = Cl(4) for Sn(4) in **3**; X = O(1), Y = O(3) for Sn(2) in **6**; X = O(3), Y = Cl(1) for Sn(3) and X = O(4), Y = Cl(2) for Sn(4) in **8**[23]) in the case of the exocyclic tin atoms.

For the exocyclic tin atoms, the distortion from the ideal trigonal-bipyramidal configuration is reflected in the axial angles X−Sn−Y ranging from 167.14(5)° (**3**; X = Cl(2), Y = Cl(4)) to 158.49(18)° (**6**; X = O(1), Y = O(3)) and in the equatorial C−Sn−C angles falling between 119.4° (**8**[23]) and 128.7° (**3**). For the endocyclic tin atoms, the corresponding axial X−Sn−O angles deviate even more from the ideal value of 180° and range from 156.37(10)° (**3**; X = Cl(1)) to 146.59(15)° (**6**; X = O(1)), whereas the equatorial C−Sn−C angles are 130.1(2)/132.9(3)° for **3**, 119.7(3)° for **6**, and 142.9(9)/139.4(10)° for **8**.[23] The widening of the C−Sn−C angles for compounds **3** and **8**[23] is the result of intramolecular Sn···Cl distances of 3.6477(17)/3.6161(19) and 3.580/3.702 Å, respectively, being shorter than the sum of the van der Waals radii[52b] of tin (2.20 Å) and chlorine (1.7−1.9 Å). This effect is even more pronounced for the related unsymmetrically substituted tetraorganodistannoxane $[t\text{-}Bu_2(Cl)SnOSn(Cl)CH_2SiMe_3]_2$ (C−Sn−C = 146.7(2)°, Sn···Cl = 3.115(2) Å).[29] In contrast to compound **6**, with an intramolecular Sn···OH distance of 3.583(5) Å being close to the sum of the van der Waals radii[52b] of tin and oxygen (1.50 Å) and being associated with a C−Sn−C angle of 119.7(3)° (see above), the shortening of this distance to 3.429(11) Å in the related derivative $[t\text{-}Bu_2(OH)SnOSn(OH)CH_2SiMe_3]_2$[29] is suf-

Table 5. Selected Bond Lengths (Å) and Angles (deg) for 7

Sn(1)−O(1)	1.961(2)	Sn(1)−O(3)	1.966(3)
Sn(1)−C(1)	2.127(4)	Sn(1)−C(11)	2.125(4)
Sn(2)−O(1)	1.966(3)	Sn(2)−O(2)	1.965(3)
Sn(2)−C(21)	2.144(4)	Sn(2)−C(31)	2.129(4)
Sn(3)−O(2)	1.962(3)	Sn(3)−O(3)	1.980(2)
Sn(3)−C(41)	2.133(4)	Sn(3)−C(51)	2.120(4)
O(1)−Sn(1)−O(3)	101.73(11)	O(1)−Sn(1)−C(1)	109.24(14)
O(1)−Sn(1)−C(11)	108.18(13)	O(3)−Sn(1)−C(1)	109.52(14)
O(3)−Sn(1)−C(11)	110.71(15)	C(1)−Sn(1)−C(11)	116.43(18)
O(1)−Sn(2)−O(2)	104.04(11)	O(1)−Sn(2)−C(21)	109.07(14)
O(1)−Sn(2)−C(31)	105.14(15)	O(2)−Sn(2)−C(21)	105.80(14)
O(2)−Sn(2)−C(31)	111.28(13)	C(21)−Sn(2)−C(31)	120.38(16)
O(2)−Sn(3)−O(3)	103.83(11)	O(2)−Sn(3)−C(41)	105.91(14)
O(2)−Sn(3)−C(51)	108.59(15)	O(3)−Sn(3)−C(41)	108.83(14)
O(3)−Sn(3)−C(51)	110.48(13)	C(41)−Sn(3)−C(51)	118.16(16)
Sn(1)−O(1)−Sn(2)	122.93(13)	Sn(1)−O(3)−Sn(3)	122.10(12)
Sn(2)−O(2)−Sn(3)	122.29(14)		
Sn(1)−O(1)−Sn(2)−O(2)	−60.06(17)	O(1)−Sn(2)−O(2)−Sn(3)	25.44(17)
Sn(2)−O(2)−Sn(3)−O(3)	23.91(17)	O(2)−Sn(3)−O(3)−Sn(1)	−60.90(18)
Sn(3)−O(3)−Sn(1)−O(1)	34.38(18)	O(3)−Sn(1)−O(1)−Sn(2)	31.34(18)

Table 6. Selected Solution ($CDCl_3$) and Solid-State ^{119}Sn NMR Chemical Shifts of 1−8

compd (R = CH_2SiMe_3)	$\delta(^{119}Sn)$	$\delta(^{119}Sn$ MAS)
R_2SnCl_2 (**1**), $R_2SnCl_2 \cdot H_2O$ (**1a**)	146.6 (**1**)	−53.9 (**1a**)
R_2SnBr_2 (**2**)	68.3	77.9
$[R_2(Cl)SnOSn(Cl)R_2]_2$ (**3**)	−60.1,[a] −133.5[b]	−28.4, −54.6, −124.0, −131.6
$[R_2(HO)SnOSn(Br)R_2]_2$ (**4**)	−155.2,[c] −171.2[d]	−159.6, −169.5, −176.9, −186.4
$[R_2(F)SnOSn(Br)R_2]_2$ (**5**)	−118.4,[e] −131.3[f]	−110.3,[g] −156.8[h]
$[R_2(HO)SnOSn(OH)R_2]_2$ (**6**)	−141.2,[i] −155.0[i]	−143.8, −162.6
$(R_2SnO)_3$ (**7**)	48.2[j]	46.6,[k] 49.5,[l] 68.5[m]
$[R_2(HO)SnOSn(Cl)R_2]_2$ (**8**)	−147.0,[n] −153.9[o]	>4 signals[p]

[a] $^2J(^{119}Sn-O-^{119/117}Sn)$ = 73 Hz. [b] $^2J(^{119}Sn-O-^{119/117}Sn)$ = 77 Hz. [c] $\nu_{1/2}$ = 50 Hz, $^2J(^{119}Sn-O-^{119/117}Sn)$ = 210 Hz. [d] $\nu_{1/2}$ = 15 Hz, $^2J(^{119}Sn-O-^{119/117}Sn)$ = 213 Hz. [e] Doublet; $^1J(^{119}Sn-^{19}F)$ = 988 Hz; $^2J(^{119}Sn-O-^{119/117}Sn)$ = 196 Hz. [f] Doublet of doublets, $^1J(^{119}Sn-^{19}F)$ = 1560 Hz; $^2J(^{119}Sn-O-^{119/117}Sn)$ = 203 Hz, $^3J(^{119}Sn-OSn-^{19}F)$ = 30 Hz. [g] Doublet; $^1J(^{119}Sn-^{19}F)$ = 854 Hz. [h] Doublet; $^1J(^{119}Sn-^{19}F)$ = 1617 Hz. [i] $\nu_{1/2}$ = 400 Hz. [j] $^2J(^{119}Sn-O-^{117}Sn)$ = 335 Hz. [k] $^2J(^{119}Sn-O-^{119/117}Sn)$ = 299 Hz. [l] $^2J(^{119}Sn-O-^{119/117}Sn)$ = 281 Hz. [m] $^2J(^{119}Sn-O-^{119/117}Sn)$ = 274 Hz. [n] $^2J(^{119}Sn-O-^{119/117}Sn)$ = 77 Hz. [o] $^2J(^{119}Sn-O-^{119/117}Sn)$ = 77 Hz. [p] Possibly a result of different crystal modifications.

ficient to cause a widening of the corresponding C−Sn−C angle in the latter derivative to 134.3(6)°.

The Sn(endo)−X−Sn(exo) bridges are unsymmetric, with distances of 2.5775(15)/2.9206 and 2.5865(16)/2.8574(16) Å for **3** (X = Cl(1), Cl(2)), 2.147(4)/2.342(4) Å for **6** (X = O(1)), and 2.26(2)/2.32(2) and 2.24(2)/2.40(2) Å for **8**[23] (X = O(3), O(4)). The asymmetry of the axial Sn−X and Sn−Y bonds amounts to 0.5266 and 0.4437 Å for **3** (X = Cl(1), Y = Cl(3) and X = Cl(2), Y = Cl(4)), 0.3100 Å for **6** (X = O(1), Y = O(3)), and 0.20 and 0.09 Å for **8**[23] (X = Cl(1), Y = O(3) and X = Cl(2) and Y = O(4)), while the asymmetry of the axial Sn−X and Sn−O bonds amounts to 0.3745 and 0.3955 Å for **3** (X = Cl(1), Cl(2)), 0.018 Å for **6** (X = O(1)), and 0.09 and 0.08 Å for **8**[23] (X = O(3), O(4)).

^{119}Sn NMR Spectroscopy. The ^{119}Sn NMR chemical shifts in solution ($CDCl_3$) and the solid state of compounds **1**−**8** are listed in Table 6. For the bis((trimethylsilyl)methyl)tin species ^{119}Sn NMR chemical shifts in solution are found between 146.6 (**1**) and 48.2 ppm (**7**) for tetracoordinated tin atoms and between −60.1 (**3**) and −170.0 ppm (**4**) for pentacoordinated tin atoms. The sensitivity of the ^{119}Sn chemical shift to the coordination number is further demonstrated by comparing $(Me_3SiCH_2)_2SnCl_2$ (**1**) and the corresponding water adduct $(Me_3SiCH_2)_2SnCl_2 \cdot H_2O$ (**1a**), which show signals at 146.6 ppm (in solution) and −53.9 ppm (in the solid state), a remarkable difference of 200.5 ppm. In solution tetraorganodistannoxanes reveal two distinct ^{119}Sn NMR signals, the chemical shifts of which are quite different for $[R_2(Cl)SnOSn(Cl)R_2]_2$ (**3**; R = CH_2SiMe_3) and relatively similar for dimeric tetraorganodistannoxanes containing hydroxy groups (**4**, **6**, and **8**). In the former compound, the high- and low-frequency signals are unambiguously assigned to the exo- and endocyclic tin atoms, respectively.[53,54] For the latter such an assignment would be less straightforward.[53,54] However, on the basis of a comparison of the ^{119}Sn NMR chemical shifts of **6** and **8** with the ^{119}Sn MAS chemical shifts of the related dimeric tetraorganodistannoxanes $[t\text{-}Bu_2(X)SnOSn(Y)R_2]_2$ (X = Cl, Y = OH; X = Y = OH; R = CH_2SiMe_3), a tentative assignment of the respective low-frequency signals to the endocyclic tin atoms is possible.[30]

Electrospray Mass Spectrometry. Electrospray mass spectra (negative mode, moist acetonitrile) were recorded in order to identify anionic diorganotin species related to $(Me_3SiCH_2)_2SnCl_2$ (**1**) and $[R_2(Cl)SnOSn(Cl)R_2]_2$ (**3**; R = CH_2SiMe_3) by partial hydrolysis or autoionization in highly polar solvents. These anionic diorganotin species can be regarded as missing links between the isolated hydrolysis products described above and in previous works and, on the other hand, the collection of diorganotin species identified in aqueous solutions by Tobias et al.[2−7] For $(Me_3SiCH_2)_2SnCl_2$ (**1**) the anionic diorganotin species **9a**−**c** and for $[R_2(Cl)SnOSn(Cl)R_2]_2$ (**3**; R = CH_2SiMe_3) the anionic diorganotin species **9a**,**c**, **10a**,**b**, and **11a**−**c** were identified (Chart 2). Notably, in contrast to the results found for diorganotin dichlo-

(53) Otera, J.; Yano, T.; Nakashima, K.; Okawara, R. *Chem. Lett.* **1984**, 2109.
(54) Yano, T.; Nakashima, K.; Otera, J.; Okawara, R. *Organometallics* **1985**, *4*, 1501.

Chart 2

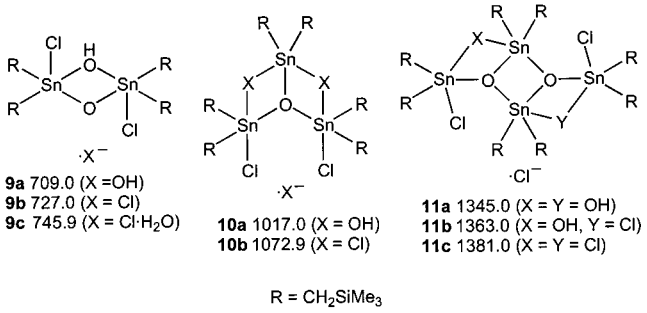

rides containing smaller organic substituents, such as Me_2SnCl_2 or Et_2SnCl_2, no mass clusters with more than four tin atoms were observed.[55]

Proposed Hydrolysis Pathway. The isolated and in situ identified diorganotin species in the present and previous works[9−25] allow the development of a scheme for the hydrolysis pathway of a diorganotin dichloride containing reasonably bulky substituents such as the (trimethylsilyl)methyl group (Scheme 2). Typically, these hydrolysis reactions are carried out in two-layer mixtures consisting of an organic solvent and aqueous base. Since neutral diorganotin species containing more than one tin atom are virtually insoluble in aqueous solutions,[8] it appears likely that small compounds with a high solubility in both nonpolar organic solvents and water play a predominant role for the actual hydrolysis steps. These small compounds are believed to migrate between the layers and apparently to autoassociate in the polar aqueous layer.[2−7] Thus, the initial step in the hydrolysis of a diorganotin dichloride R_2SnCl_2 (**I**) involves the substitution of a chlorine atom by a hydroxy group to give the diorganotin hydroxide chloride $R_2Sn(OH)Cl$ (**II**). Mechanistically, the substitution presumably proceeds via nucleophilic attack of **I** in the aqueous layer by a hydroxide ion or a water molecule, followed by the formation of a pentacoordinated intermediate, $[R_2SnCl_2{\cdot}OH]^-$ or $R_2SnCl_2{\cdot}H_2O$, respectively.[56] The water adduct $(Me_3SiCH_2)_2SnCl_2{\cdot}H_2O$ (**1a**) can be regarded as such an intermediate. Migrated back into the organic layer, the diorganotin hydroxide chloride $R_2Sn(OH)Cl$ (**II**) may be stabilized by dimerization, giving rise to the hydroxy-bridged four-membered ring $[R_2Sn(OH)Cl]_2$ (**III**), or condense and self-assemble to the dimeric tetraorganodistannoxane $[R_2(Cl)SnOSn(Cl)R_2]_2$ (**IV**). Di-*tert*-butyltin hydroxide chloride $[t\text{-}Bu_2Sn(OH)Cl]_2$[39] represents a well-defined example for the former class of compounds. Failed attempts at obtaining a reasonable ^{119}Sn NMR spectrum ($CDCl_3$) of $[t\text{-}Bu_2Sn(OH)Cl]_2$ can tentatively be attributed to a monomer−dimer equilibrium taking place in solution. Although no direct evidence exists for an equilibrium between $[R_2Sn(OH)Cl]$ (**II**), $[R_2(Cl)SnOSn(Cl)R_2]_2$ (**IV**), and water, a similar equilibrium for the closely related $Bu_2Sn(OH)(NO_3)$ with $[Bu_2(NO_3)SnOSn(NO_3)Bu_2]_2$ was indeed observed.[57] In the next step along the hydrolysis pathway the tetraorganodistannoxane $[R_2(Cl)SnOSn(Cl)R_2]_2$ (**IV**) dissociates into a three-quarter ladder $R_2Sn(OSnR_2Cl)_2$ (**V**) and R_2SnCl_2 (**I**). Recently, $t\text{-}Bu_2Sn(OSn\textit{t}\text{-}Bu_2Cl)_2$ was identified in solution by ^{119}Sn NMR spectroscopy as an example of a three-quarter ladder.[58] Subsequently, the three-quarter ladder $R_2Sn(OSnR_2Cl)_2$ (**V**) reacts with the diorganotin hydroxide chloride $R_2Sn(OH)Cl$ (**II**) to produce the unsymmetrically substituted tetraorganodistannoxane $[R_2(Cl)SnOSn(Cl)R_2][R_2(Cl)SnOSn(OH)R_2]$ (**VI**). In a recent conference contribution spectroscopic evidence was presented for the existence of $[Bu_2(Cl)SnOSn(Cl)Bu_2][Bu_2(Cl)SnOSn(OH)Bu_2]$,[34] and an analogue of the latter, namely $[Bu_2(Cl)SnOSn(Cl)Bu_2][Bu_2(Cl)SnOSn(OMe)Bu_2]$, was reported by Gross.[35] The replacement of the diorganotin dichloride moiety R_2SnCl_2 in **VI** by a diorganotin hydroxide chloride R_2-

Scheme 2

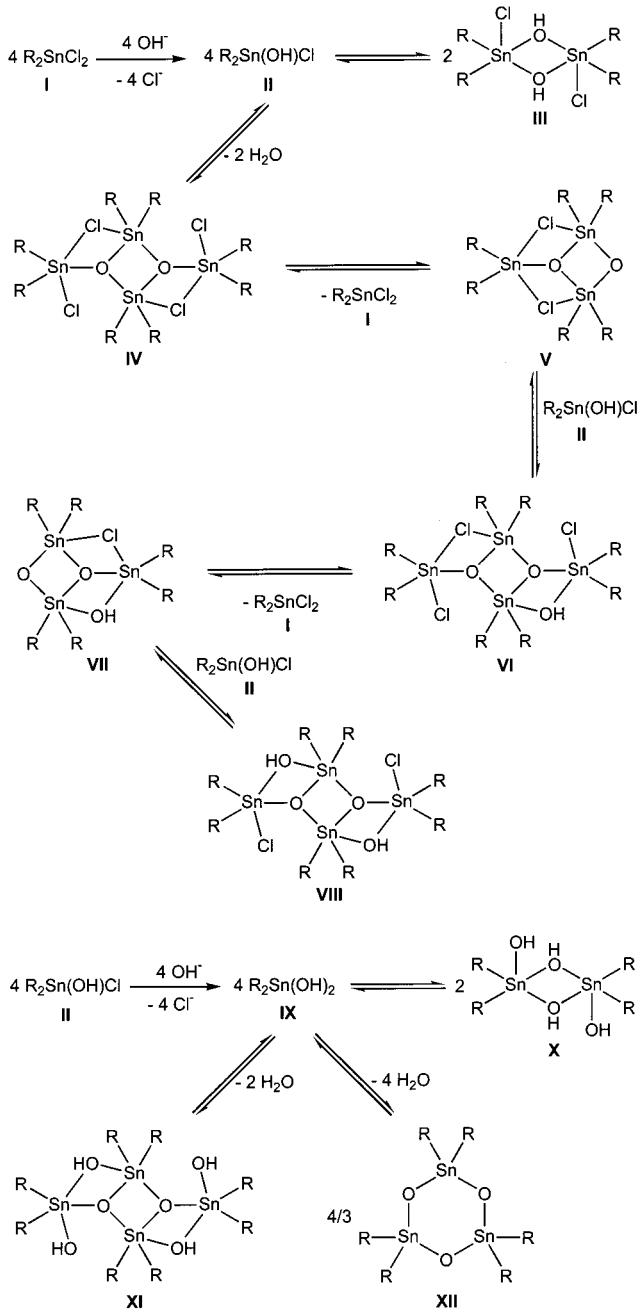

(55) Beckmann, J.; Jurkschat, K.; Kaltenbrunner, U.; Rabe, S.; Schürmann, M.; Dakternieks, D.; Duthie, A.; Müller, D. *Organometallics* **2000**, *19*, 4887.

(56) Britton, D.; Dunitz, J. D. *J. Am. Chem. Soc.* **1981**, *103*, 2971.

(57) Yasuda, K.; Matsumoto, H.; Okawara, R. *J. Organomet. Chem.* **1966**, *6*, 528.

(58) Dakternieks, D.; Jurkschat, K.; van Dreumel, S.; Tiekink, E. R. T. *Inorg. Chem.* **1997**, *36*, 2023.

Sn(OH)Cl unit (**II**) to produce the tetraorganodistannoxane $[R_2Sn(HO)SnOSn(Cl)R_2]_2$ (**VIII**) again proceeds via the unsymmetrically substituted three-quarter ladder $R_2Sn(OSnR_2Cl)(OSnR_2OH)$ (**VII**). Further hydrolysis of the diorganotin hydroxide chloride $R_2Sn(OH)Cl$ (**II**) apparently occurs in the aqueous layer, providing a diorganotin dihydroxide, $R_2Sn(OH)_2$ (**IX**), which having migrated back into the organic layer may oligomerize with or without condensation to give the dimeric diorganotin dihydroxide $[R_2Sn(OH)_2]_2$ (**X**), the dimeric tetraorganodistannoxane $[R_2(HO)SnOSn(OH)R_2]_2$ (**XI**), or finally a diorganotin oxide. This diorganotin oxide happens to be in most cases a trimer, *cyclo*-$(R_2SnO)_3$ (**XII**);[42] however, it can also be polymeric[59] or dimeric,[60] provided the organic substituents are small or very bulky, respectively. Accordingly, for $R = (Me_3Si)_2CH$ the tetraorganodistannoxane $R_2(HO)SnOSn(OH)R_2$ was found to be monomeric, even in the solid state.[60]

Experimental Section

General Data. Solvents were dried and freshly distilled prior to use. Air-sensitive compounds were handled under vacuum or nitrogen using standard vacuum line and Schlenk techniques. $(Me_3SiCH_2)_2SnPh_2$ was synthesized according to a literature procedure.[43] Solution ^1H, ^{13}C, ^{19}F, ^{29}Si, and ^{119}Sn NMR spectra were recorded on a Bruker DRX 400 or DPX 300 instrument at 400.13 (^1H), 100.31 (^{13}C), 282.40 (^{19}F), 79.49 (^{29}Si), and 149.20 MHz (^{119}Sn) in $CDCl_3$ (unless otherwise stated) and were referenced to $SiMe_4$ (^1H, ^{13}C, ^{29}Si), $CFCl_3$ (^{19}F), or $SnMe_4$ (^{119}Sn). ^{119}Sn MAS NMR spectra were obtained from a Bruker MSL 400 spectrometer using cross-polarization and high-power proton decoupling. Tetracyclohexyltin was used as a second reference (δ −97.35 ppm with respect to $SnMe_4$). The elemental analyses were performed on an instrument from Carlo Erba Strumentazione (Model 1106). FT infrared spectra were recorded using a Bruker IFS28 spectrometer. Electrospray mass spectra were obtained with a Platform II single-quadrupole mass spectrometer (Micromass, Altrincham, U.K.) using an acetonitrile mobile phase. Acetonitrile solutions (0.1 mM) of the compounds were injected directly into the spectrometer via a Rheodyne injector equipped with a 50 μL loop. A Harvard 22 syringe pump delivered the solutions to the vaporization nozzle of the electrospray ion source at a flow rate of 10 μL min^{-1}. Nitrogen was used both as a drying gas and for nebulization with flow rates of approximately 200 and 20 mL min^{-1}, respectively. Pressure in the mass analyzer region was usually about 4×10^{-5} mbar. Typically 10 signal-averaged spectra were collected.

Synthesis of Bis((trimethylsilyl)methyl)tin Dichloride (1) and Dibromide (2). Gaseous hydrogen chloride or bromide was bubbled through a solution of $(Me_3SiCH_2)_2SnPh_2$ (typically 10 g) in toluene (150 mL) at 0 °C for 4 h. The solvent was removed under vacuum, and the crude product was purified by Kugelrohr distillation. The yields were almost quantitative.

$(Me_3SiCH_2)_2SnCl_2$ (**1**) is a colorless oil. ^1H NMR: δ 0.79 (4H, s; $^2J(^1H-C-^{119}Sn) = 91$ Hz; CH_2Sn), 0.17 (18H, s; SiMe_3). ^{13}C NMR: δ 13.0 ($^1J(^{13}C-^{119}Sn) = 328$ Hz; CH_2Sn), 1.0 (SiMe_3). ^{29}Si NMR: δ 3.1 ($^2J(^{29}Si-C-^{119/117}Sn) = 38$ Hz). ^{119}Sn NMR: δ 146.6.

$(Me_3SiCH_2)_2SnCl_2$ (**1**) rapidly reacts with air moisture to give quantitatively $(Me_3SiCH_2)_2SnCl_2 \cdot H_2O$ (**1a**) as a colorless crystalline solid (mp 48−49 °C). ^{119}Sn MAS NMR: δ −53.9. IR (KBr): ν_{OH} 3649 cm^{-1}. Anal. Calcd for $C_8H_{24}Cl_2OSi_2Sn$ (382.09): C, 25.15; H, 6.33; Found: C, 24.9; H, 6.6.

$(Me_3SiCH_2)_2SnBr_2$ (**2**) is a colorless crystalline solid (mp 68 °C). ^1H NMR: δ 1.01 (4H, s; $^2J(^1H-C-^{119}Sn) = 89$ Hz; CH_2Sn), 0.20 (18H, s; SiMe_3). ^{13}C NMR: δ 14.0 ($^1J(^{13}C-^{119}Sn) = 296$ Hz; CH_2Sn), 1.0 (SiMe_3). ^{29}Si NMR: δ 3.4 ($^2J(^{29}Si-C-^{117/119}Sn) = 37$ Hz). ^{119}Sn NMR: δ 68.3. Anal. Calcd for $C_8H_{22}Br_2Si_2Sn$ (452.98): C, 21.21; H, 4.90; Found: C, 21.3; H, 5.4.

Synthesis of Bis(tetrakis((trimethylsilyl)methyl)dichlorodistannoxane) (3). To a mixture of **1** (3.64 g, 10.0 mmol) and triethylamine (1.01 g, 10.0 mmol) in diethyl ether (400 mL) was added water (90 mg, 5.0 mmol). Immediately, a voluminous precipitate of triethylammonium chloride appeared, which was filtered after 12 h. The solvent was completely removed under vacuum to leave a residue that was recrystallized from hexane to deposit **3** as a colorless crystalline solid (2.96 g, 2.20 mmol, 88%, mp 194 °C). ^1H NMR: δ 0.99 (8H, s, $^2J(^1H-C-^{117/119}Sn) = 121$ Hz; CH_2Sn), 0.96 (8H, s, $^2J(^1H-C-^{117/119}Sn) = 119$ Hz; CH_2Sn), 0.24, 0.20 (72H, s; SiMe_3). ^{13}C NMR: δ 20.9 ($^1J(^{13}C-^{119}Sn) = 515$ Hz; CH_2Sn), 20.5 ($^1J(^{13}C-^{119}Sn) = 457$ Hz; CH_2Sn), 2.1, 1.5 (SiMe_3). ^{29}Si NMR: δ 1.7, 1.4. ^{119}Sn NMR: δ −60.1 ($^2J(^{119}Sn-O-^{117/119}Sn) = 73$ Hz), −133.5 ($^2J(^{119}Sn-O-^{117/119}Sn) = 77$ Hz). ^{119}Sn MAS NMR: δ −28.4, −54.6, −124.0, −131.6. IR (KBr): ν_{OH} 3645 cm^{-1}. Anal. Calcd for $C_{32}H_{88}Cl_4Si_8Sn_4O_2$ (1346.48): C, 28.55; H, 6.59; Cl, 10.53. Found: C, 28.8; H, 6.8; Cl, 10.4.

Synthesis of Bis(tetrakis((trimethylsilyl)methyl)bromohydroxydistannoxane (4). To a solution of **2** (18.1 g, 40.0 mmol) in boiling toluene (300 mL) was added dropwise a solution of sodium hydroxide (2.4 g, 60.0 mmol) in water. The reaction mixture was heated at reflux for 5 h. After the mixture was cooled to room temperature, the layers were separated and the organic layer dried over Na_2SO_4. The solvent was evaporated until the crystallization started. Compound **4** crystallized as a colorless solid at −10 °C (10.3 g, 7.4 mmol, 74%, mp 195 °C). ^1H NMR: δ 1.01 (16H, s, $^2J(^1H-C-^{119}Sn) = 89.2$ Hz; CH_2Sn), 0.20 (72H, s; SiMe_3). ^{13}C NMR: δ 18.0 ($^1J(^{13}C-^{119}Sn) = 501$ Hz; SnCH_2), 15.0 ($^1J(^{13}C-^{119}Sn) = 525$ Hz; SnCH_2), 2.3, 1.8 (SiMe_3). ^{29}Si NMR: δ 1.7, 1.5. ^{119}Sn NMR: δ −155.2 (2Sn, $^2J(^{119}Sn-^{117}Sn) = 210$ Hz), −171.2 (2Sn, $^2J(^{119}Sn-^{117}Sn) = 213$ Hz). ^{119}Sn MAS NMR: δ −159.6, −169.5, −176.9, −186.4. IR: ν_{OH} 3643 cm^{-1}. Anal. Calcd for $C_{32}H_{90}Br_2O_4Si_8Sn_4$ (1398.50): C, 27.48; H, 6.49; Br, 11.43. Found: C, 27.9; H, 6.9; Br, 11.3.

Synthesis of Bis(tetrakis((trimethylsilyl)methyl)bromofluorodistannoxane) (5). To a solution of **2** (18.1 g, 40.0 mmol) in boiling toluene (300 mL) was added dropwise an aqueous solution of sodium hydroxide (2.40 g, 60 mmol) and sodium fluoride (1.26 g, 30 mmol). After it was heated at reflux for 12 h, the reaction mixture was cooled to room temperature and the organic layer was separated and dried over Na_2SO_4. After filtration the solvent was evaporated and the residue recrystallized from hexane to give **6** as a colorless crystalline solid (9.4 g, 6.7 mmol, 67%, mp. 175 °C). ^1H NMR: δ 0.71 (4H, d, $^2J(^1H-C-^1H) = 9$ Hz; CH_2Sn), 0.70 (4H, d, $^2J(^1H-C-^1H) = 12$ Hz; CH_2Sn), 0.69 (4H, d, $^2J(^1H-C-^1H) = 9$ Hz; CH_2Sn), 0.62 (4H, d, $^2J(^1H-C-^1H) = 12$ Hz; CH_2Sn), 0.10, 0.09 (72H, s; SiMe_3). ^{13}C NMR: δ 16.3 (d, $^2J(^{13}C-Sn-^{19}F) = 10$ Hz, $^1J(^{13}C-^{119}Sn) = 477$ Hz; CH_2Sn), 14.6 (d, $^2J(^{13}C-Sn-^{19}F) = 14$ Hz, $^1J(^{13}C-^{119}Sn) = 460$ Hz; CH_2Sn), 2.0, 1.6 (SiMe_3). ^{19}F NMR: δ −78.9 ($^1J(^{19}F-^{119}Sn) = 1554$ Hz, $^1J(^{19}F-^{117/119}Sn) = 976$ Hz) and minor signals (see text). ^{29}Si NMR: δ 2.1, 2.0. ^{119}Sn NMR: δ −118.4 (d, $^1J(^{119}Sn-^{19}F) = 988$ Hz, $^2J(^{119}Sn-O-^{117}Sn) = 196$ Hz), −131.3 (d, $^1J(^{119}Sn-^{19}F) = 1560$ Hz, $^2J(^{119}Sn-O-^{117}Sn) = 203$ Hz, $^3J(^{119}Sn-OSn-^{19}F) = 30$ Hz) and minor signals (see text). ^{119}Sn MAS NMR: δ −110.3 (2Sn, d, $^1J(^{119}Sn-^{19}F) = 854$ Hz), −156.8 (2Sn, d, $^1J(^{119}Sn-^{19}F) = 1617$ Hz). Anal. Calcd for $C_{32}H_{88}Br_2F_2O_2Si_8Sn_4$ (1402.48): C, 27.41; H, 6.32; Br, 11.40; Found: C, 27.5; H, 6.6; Br, 10.5.

Synthesis of Bis(tetrakis((trimethylsilyl)methyl)dihydroxydistannoxane) (6). To a solution of **4** (5.59 g, 4.00

(59) Ingham, R. K.; Rosenberg, S. D.; Gilman, H. *Chem. Rev.* **1960**, *60*, 459.
(60) Edelman, M. A.; Hitchcock, P. B.; Lappert, M. F. *J. Chem. Soc., Chem. Commun.* **1990**, 1116.

mmol) in boiling toluene (150 mL) was added dropwise a solution of sodium hydroxide (4.0 g, 10.0 mmol) in water. The reaction mixture was heated at reflux for 12 h. After the mixture was cooled to room temperature, the organic layer was separated and dried over Na_2SO_4. After filtration the solvent was reduced under vacuum to a volume of approximately 20 mL. This solution was left in an open flask (air moisture) at room temperature to give **6** as a colorless crystalline solid (2.95 g, 2.32 mmol, 58%, mp 178 °C). ^{1}H NMR: δ 0.28 (16H, s; CH_2-Sn), 0.12 (72H, s; SiMe_3). ^{13}C NMR: δ 11.4 (CH_2Sn), 1.8 (SiMe_3). ^{29}Si NMR: δ 1.4. ^{119}Sn NMR: δ −141.2 ($\nu_{1/2}$ = 400 Hz), −155.0 ($\nu_{1/2}$ = 400 Hz), and a minor signal related to **7**. ^{119}Sn MAS NMR: δ −143.8, −162.6. IR (KBr): ν_{OH} 3656 s cm^{-1}. Anal. Calcd for $C_{32}H_{92}O_6Si_8Sn_4$ (1272.70): C, 30.20; H, 7.29. Found: C, 30.3; H, 8.4.

Synthesis of Hexakis((trimethylsilyl)methyl)cyclotristannoxane (7). A solution of **6** (2.54 g, 2.00 mmol) in toluene (50 mL) was heated at reflux for 5 h, followed by addition of freshly activated molecular sieves (4 Å, 10 g). The mixture was heated again for 2 h, the molecular sieves were removed by filtration, and the solvent of the filtrate was evaporated under vacuum. The residual oil solidified slowly at −10 °C, giving **7** as a colorless crystalline solid (2.37 g, 2.56 mmol, 96%, mp 43 °C). ^{1}H NMR: δ 0.23 (12H, s, ^2J(^{1}H−^{119}Sn) = 91 Hz; CH_2Sn), 0.10 (54H, s; SiMe_3). ^{13}C NMR: δ 8.8 (^1J(^{13}C−^{119}Sn) = 380 Hz; CH_2Sn), 1.7 (SiMe_3). ^{29}Si NMR: δ 1.2 (^2J(^{29}Si−C−$^{117/119}$Sn) = 26 Hz). ^{119}Sn NMR: δ 48.2 (^2J(^{119}Sn−O−^{117}Sn) = 335 Hz). ^{119}Sn MAS NMR: δ 68.5 (^2J(^{119}Sn−O−$^{117/119}$Sn) = 299 Hz), 49.5 (^2J(^{119}Sn−O−$^{117/119}$Sn) = 281 Hz), 46.6 (^2J(^{119}Sn−O−$^{117/119}$Sn) = 274 Hz). Anal. Calcd for $C_{24}H_{66}O_3Si_6Sn_3$ (927.50): C, 31.08; H, 7.17. Found: C, 31.1; H, 7.3.

Synthesis of bis(tetrakis(trimethylsilylmethyl)chlorohydroxydistannoxane) (8). A mixture of **3** (1.35 g, 1.0 mmol) and **6** (1.27 g, 1.0 mmol) in toluene (20 mL) was heated to 60 °C for 2 h. After the mixture was cooled, the solvent was evaporated and the residue recrystallized from hexane, giving **8** as a colorless crystalline solid (2.62 g, 2.0 mmol, 100%, mp 194 °C). ^{1}H NMR: δ 0.75 (4H, d, ^2J(^{1}H−C−^{1}H) = 8 Hz; CH_2-Sn), 0.71 (4H, d, ^2J(^{1}H−C−^{1}H) = 11 Hz; CH_2Sn), 0.68 (4H, d, ^2J(^{1}H−C−^{1}H) = 8 Hz; CH_2Sn), 0.63 (4H, d, ^2J(^{1}H−C−^{1}H) = 11 Hz; CH_2Sn), 0.11, 0.01 (72H, s; SiMe_3). ^{13}C NMR: δ 16.0 (^1J(^{13}C−^{119}Sn) = 479 Hz; CH_2Sn), 13.9 (^1J(^{13}C−^{119}Sn) = 482 Hz; CH_2Sn), 2.1, 1.7 (SiMe_3). ^{29}Si NMR: δ 1.3, 1.1. ^{119}Sn NMR: δ −147.0 (^2J(^{119}Sn−O−^{117}Sn) = 215 Hz), −153.9 (^2J(^{119}Sn−O−^{117}Sn) = 220 Hz). ^{119}Sn MAS NMR: more than four signals (see text). IR: ν_{OH} 3654 cm^{-1}. Anal. Calcd for $C_{32}H_{90}Cl_2O_4Si_8Sn_4$ (1309.59): C, 29.35; H, 6.93. Found: C, 29.4; H, 7.2.

Crystallography. Intensity data for the colorless crystals were collected on a Nonius KappaCCD diffractometer with graphite-monochromated Mo Kα (0.71069 Å) radiation at 291 K. The data collection covered almost the whole sphere of reciprocal space with 360 frames via ω-rotation (Δ/ω = 1°) at 2 times 10 s (**3**, **6**, **7**), and 90 s (**1a**) per frame. The crystal-to-detector distances were 2.7 cm (**1a**, **3**) and 2.80 cm (**6**, **7**). Crystal decay was monitored by repeating the initial frames at the end of data collection. Analyzing the duplicate reflections showed there was no indication for any decay. The data were not corrected for absorption effects. The structure was solved by direct methods using SHELXS97[61] and successive difference Fourier syntheses. Refinement involved full-matrix least-squares methods using SHELXL97.[62] The H atoms were placed in geometrically calculated positions using a riding model (O−H = 0.82 Å, C−H$_{prim}$ = 0.96 Å, C−H$_{sec}$ = 0.97 Å) and refined with common isotropic temperature factors (U_{iso} = 0.13(1) Å^2 (**1a**), 0.170(4) Å^2 (**3**), 0.128(3) (**7**) Å^2). The isotropic temperature factors of the H atoms of **6** are constrained to be 1.5 times those of the carrier atom. A disordered (trimethylsilyl)methyl group (**6**) was found with occupancies of 0.5 (C(2), C(2′)). A racemic twin refinement was applied at the end of refinement, because of the Flack[63] parameter value of 0.50(4) in the preceding refinements. Atomic scattering factors for neutral atoms and real and imaginary dispersion terms were taken from ref 64. The figures were created by SHELXTL.[65] Crystallographic data are given in Table 1 and selected bond distances and angles for **1a** in Table 2, for **3** in Table 3, for **6** in Table 4, and for **7** in Table 5.

Acknowledgment. We thank the Deutsche Forschungsgemeinschaft and the Fonds der Chemischen Industrie for financial support.

Supporting Information Available: Tables of all coordinates, anisotropic displacement parameters, and geometric data for compounds **1a**, **3**, **6**, and **7**. This material is available free of charge via the Internet at http://pubs.acs.org.

OM010715Q

(61) Sheldrick, G. M. *Acta Crystallogr.* **1990**, *A46*, 467.
(62) Sheldrick, G. M. University of Göttingen, 1997.
(63) Flack, H. D. *Acta Crystallogr.* **1983**, *A39*, 876.
(64) *International Tables for Crystallography*; Kluwer Academic: Dordrecht, The Netherlands, 1992; Vol. C.
(65) Sheldrick, G. M. *SHELXTL, Release 5.1 Software Reference Manual*; Bruker AXS: Madison, WI, 1997.